Available online at www.sciencedirect.com
ScienceDirect
Solid State Communications 141 (2007) 6–11
solid state communications
www.elsevier.com/locate/ssc

Energy shift of photoemission spectra for organics-passivated CdSe nanoparticles: The final-state effect

Pin-Jiun Wu[a,b], Ku-Ding Tsuei[b,c,*], Kung-Hwa Wei[d], Keng S. Liang[a,b]

[a] *Department of Electrophysics, National Chiao-Tung University, Hsinchu 300, Taiwan*
[b] *National Synchrotron Radiation Research Center, Hsinchu 300, Taiwan*
[c] *Department of Physics, National Tsing-Hua University, Hsinchu 300, Taiwan*
[d] *Department of Material Science and Engineering, National Chiao-Tung University, Hsinchu 300, Taiwan*

Received 6 June 2006; received in revised form 25 September 2006; accepted 25 September 2006 by B. Jusserand
Available online 11 October 2006

Abstract

Size-dependent energy shift of photoemission spectra with respect to bulk sample has been examined for colloidally prepared CdSe nanoparticles with a series of particle sizes. The core-level shifts are well described by a theoretical calculation based on a final-state effect model, whereas an additional initial-state effect due to quantum confinement is required to elucidate the valence-band edge shifts. The results indicate that the interaction between the photohole and the dielectric background in the final state has to be considered in photoemission measurements for organics-passivated nanoparticles. The calculated results in the literature appear to overestimate the initial-state effect compared to our experimental observation.

PACS: 71.20.Nr; 73.61.Tm; 79.60.-i

Keywords: A. Nanostructures; B. Chemical synthesis; E. Photoelectron spectroscopies; E. Synchrotron radiation

1. Introduction

Nanoparticles (NPs) are objects whose physical sizes are comparable to the quantum sizes of their electronic excitations to achieve the so called quantum confinement effect [1]. With the advancement of synthesis techniques semiconductor nanoparticles of monodispersed size distribution have become available during the past twenty years allowing clear observation of this effect [2,3]. It is well known that a strong correlation exists between the size and the electronic behaviors of nanostructural materials and is the basis for the design of their tunable optical properties for applications in light-emitting diode [4,5], phosphor [6], biosensor [7,8] and so on. Since these nano-objects are composed of only several tens to thousands of atoms, to investigate the characteristics of their size-dependent electronics remains a big challenge [9–11].

Photoemission spectroscopy is a powerful tool to directly investigate the electronic structure of nanomaterials [10,11]. The electron energy measured in a photoemission experiment is in principle influenced by both the initial-state and final-state effects. The initial-state effect is related to the electronic properties of materials, and the final-state effect is ascribed to the hole final state and the possible interaction between the outgoing electron and the positively charged state left behind. In the past, the size-dependent photoemission spectra of low-dimensional metal clusters have attracted much interest [12,13]. It has been demonstrated that the final-state effect plays a dominant role in such systems [14]. Related calculations were developed to address the importance of the remaining positive charge for free clusters [15,16]. In contrast, a comprehensive understanding of the size-dependent energy shift of the core-level and valence-band photoemission spectra for the semiconductor NPs is lacking, despite the pioneering work by

* Corresponding address: National Synchrotron Radiation Research Center, 101 Hsin-Ann Rd. Hsinchu Science Park, 30076 Hsinchu, Taiwan. Tel.: +886 3 5780281x7105; fax: +886 3 5783813.
E-mail address: tsuei@nsrrc.org.tw (K.-D. Tsuei).

0038-1098/$ - see front matter © 2006 Elsevier Ltd. All rights reserved.
doi:10.1016/j.ssc.2006.09.048

Colvin et al. published long ago [11]. A more recent paper discusses only the initial-state quantum shift relative to bulk in the valence-band edge by subtracting the core-level shift [9].

We present in this paper a detailed study of the size-dependent electronic structure of organics capped CdSe NPs by use of high-resolution photoemission spectroscopy with synchrotron radiation. We show that the energy shift of core levels for TOPO/HDA passivated CdSe NPs can be well described by the electrostatic interaction of the final state involving the photohole left behind and the induced polarization. The valence-band edge shift on the other hand reveals an additional initial-state shift due to quantum confinement. Our analysis shows that a comprehensive understanding of the measured photoemission shift has to consider the final-state effect and its difference between the core level and valence band. The extracted valence-band shifts due to quantum confinement are smaller than the calculated results from the literature.

2. Experimental section

The synthesized method of CdSe NPs was according to the method reported in the literature [2,17]. Briefly, CdO was dissolved in the mixture of trioctylphosphine oxide (TOPO) and hexadecylamine (HDA), and heated to about 270 °C under argon gas. Adequate octadecylphosphonic acid (OPA) was injected into the mixture to form the Cd precursor with a color varying from dark red to transparent. Meanwhile, the Se solution was prepared by mixing Se pellets with trioctylphosphine (TOP) and maintained at 150 °C. Then TOPSe was rapidly injected into the Cd precursor. By controlling the reaction time and growth conditions, TOPO/HDA passivated CdSe NPs with various sizes can be obtained [18]. These crude products were dissolved in toluene and methanol to remove the unbounded ligands and to improve the size distribution. This purification process was repeated several times such that the high quality CdSe NPs can be achieved.

CdSe NPs with mean diameters D_m ranging from 18 to 42 Å were used in this work, where D_m is defined by $(D_{\text{major}} \times D^2_{\text{minor}})^{1/3}$, and D_{major} and D_{minor} denote the major and minor diameters of the prolate particles, respectively. The diameters of synthesized CdSe NPs were determined by x-ray powder diffraction (XPD) and transmission electron microscope (TEM), with size distribution about 5% standard deviation. Optical absorption and luminescent spectra were also checked in a solution formed by dispersing the NPs of less than 1 mg in 3 mL toluene. It is found that the relation between the optical absorption peaks and the averaged sizes is consistent with the literature [19].

Photoemission experiments using synchrotron radiation were performed at BL-08A1 and BL-24A1 of the National Synchrotron Radiation Research Center (NSRRC), Taiwan. BL-08A1 is a low-energy spherical-grating monochromator (LSGM) beamline, which provides radiation energies in the range of 20–160 eV. It was therefore used to measure the valence-band and Se 3d core-level spectra. BL-24A1 is a wide-range spherical-grating monochromator (WR-SGM) beamline offering photons up to 1500 eV, and thus was used for the measurement of the Cd 3d core-level spectra.

All NP samples for the photoemission measurements were prepared by casting dilute solution with dispersed NPs onto tantalum foil, and it was allowed to evaporate the solvent (toluene) under nitrogen gas. The samples were then transferred to the photoemission chamber in less than 10 min to minimize the chance of being oxidized. The thus-prepared samples showed no oxidized components in photoemission spectra from contamination. Pure CdSe powder adhered to a Cu foil was used as bulk reference. All NP samples, a bulk sample and a gold foil were mounted on a grounded sample holder, and the Fermi level of gold was used as reference for binding energy calibration. An Omicron EA-125 hemispherical energy analyzer was used for collecting photoelectrons at overall resolution of about 0.05–0.1 eV. A chamber base pressure of 2×10^{-9} Torr was maintained during the photoemission experiments.

3. Results and discussion

3.1. Synchrotron radiation photoemission spectra

Fig. 1 shows the Cd $3d_{5/2}$ and Se 3d core-level photoemission spectra of CdSe NPs and the corresponding fits with three mean diameters of 42, 32, and 18 Å at room temperature, as well as those of the bulk sample. A polynomial background of these spectra has been subtracted out before fitting the peaks to the least number of Voigt functions.

As shown in Fig. 1(a), all Cd $3d_{5/2}$ core-level photoemission spectra measured with a photon energy of 480 eV can be fitted with one single Voigt function. It means that the surface and bulk components of the Cd $3d_{5/2}$ core-level spectra cannot be differentiated in energy. The spectrum of bulk solids has a binding energy of 405.6 eV, in agreement with the value reported in the literature [20]. For the CdSe NPs the Cd $3d_{5/2}$ photoemission peak has a shift toward higher binding energy relative to the bulk crystallite. This shift is accompanied with a systematic increase as the particle size decreases. Moreover, these spectra exhibit a linewidth broadening resulting from increased structural disorder [21,22].

For the Se 3d core-level photoemission spectra in Fig. 1(b), a photon energy of 120 eV was chosen to have the same kinetic energy as in the Cd $3d_{5/2}$ core-level spectra, in order to probe the same depth in NPs. A good fit can be achieved by one single spin-orbit split doublet of Voigt function for the bulk sample. The obtained Se $3d_{5/2}$ peak has a binding energy of 54.4 eV, consistent with the literature value [23]. In contrast, two spin-orbit split doublets of Voigt functions were necessary to obtain fits with reliable quality for all Se 3d core-level spectra of CdSe NPs. The results reveal that the intensity of the higher binding energy component is enhanced relative to that of the lower binding energy component as the particle size decreases. Therefore, the component at higher binding energy can be assigned to the surface Se atoms of CdSe NPs due to the increase of surface to bulk atom ratio, while another component at lower binding energy is from the interior Se atoms. Similar to the tendency of energy shifts for the Cd $3d_{5/2}$ core-level spectra,

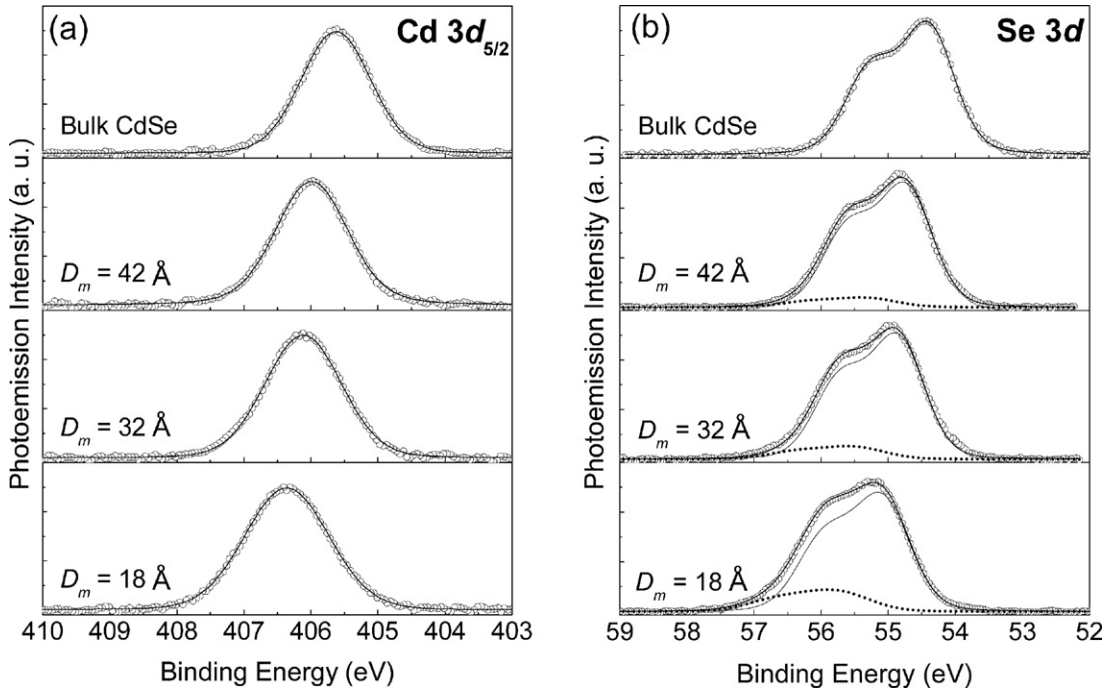

Fig. 1. Size-dependent (a) Cd $3d_{5/2}$ and (b) Se 3d photoemission spectra of bulk CdSe and TOPO/HDA passivated CdSe NPs with three mean diameters D_m were measured at room temperature with photon energies of 480 eV and 120 eV, respectively. All Cd 3d spectra show good fits by only one single component, whereas with the exception of bulk CdSe the Se 3d spectra of NP samples are composed of interior (solid lines) and surface components (dotted lines).

the interior components of the Se 3d core-level spectra for CdSe NPs shift to higher binding energy relative to that of bulk CdSe. We note that the magnitudes of these energy shifts are close to those observed from the Cd $3d_{5/2}$ core-level spectra.

Fig. 2 shows the valence-band photoemission spectra of CdSe NPs with three sizes along with the bulk spectrum, measured at a photon energy of 50 eV so as to have the same probing depth. We have verified that the organics contribute to the spectral region below about 5 eV. Hence it can be seen that the first feature below the valence-band edge purely due to NP itself sharpens as the particle size decreases reflecting the increasing quantum confinement effect. The valence-band edge is determined by extrapolating the linear part just above the edge to its intersection with a linear background. For all NP samples the valence-band edges exhibit an increase in binding energy compared to the spectrum of bulk sample. However, it is found that the energy shifts of the valence-band edge are always larger than those of the core levels, especially of the smaller NPs, indicating a non-negligible difference in shifts between the valence-band edge and core levels.

3.2. Comparison of energy shifts and a proposed model

In the three-step model of photoemission process an electron is excited to an unoccupied state leaving a hole; this photoelectron travels to the surface and across the surface into the vacuum. There will be an electrostatic interaction between the outgoing photoelectron and the system left behind and an interaction between the hole and its surrounding medium. The kinetic energy of the outgoing photoelectron is given by the sum of photon energy and the total system energy of the initial

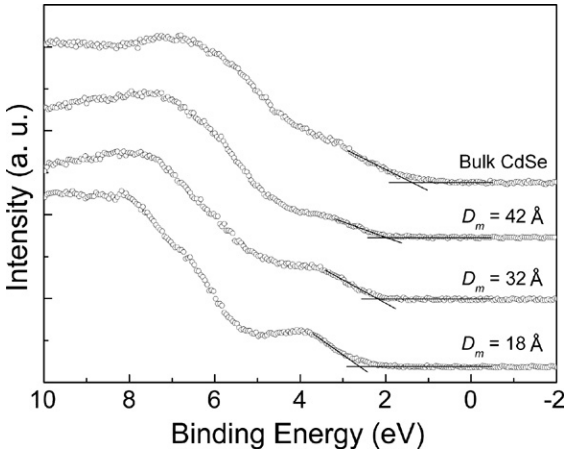

Fig. 2. Photoemission spectra for the valence band of bulk CdSe and TOPO/HDA passivated CdSe NPs with three mean diameters D_m measured at a photon energy of 50 eV at room temperature.

neutral ground state subtracted by the total system (potential) energy of the final hole state.

Here we consider a classical electrostatic model. The total potential at point $\vec{r}$ due to a point charge q at point $\vec{r}_q$, both inside a dielectric sphere with a dielectric constant ε embedded in vacuum, can be expressed as

$$\phi_{\text{in}} = \frac{q}{\varepsilon}\frac{1}{\left|\vec{r}-\vec{r}_q\right|} + \frac{q}{R}\left(\frac{\varepsilon-1}{\varepsilon}\right) \times \sum_{k=0}^{\infty}\frac{k+1}{k(\varepsilon+1)+1}\frac{r_q^k}{R^{2k}}r^k P_k(\cos\theta) \quad (1)$$

where R is the spherical radius, P_k is the Legendre polynomial, and θ is the angle between $\vec{r}$ and $\vec{r}_q$. The first term is due to the point charge directly while the second term is due to its image, or the induced polarization of the dielectric host because of its finite size. The corresponding potential outside of the dielectric sphere is

$$\phi_{\text{out}} = q \sum_{k=0}^{\infty} \frac{2k+1}{k(\varepsilon+1)+1} \frac{r_q^k}{r^{k+1}} P_k(\cos\theta). \tag{2}$$

This form ensures that the potential vanishes at infinity.

If the photoelectron travels to infinity there will be no interaction between the photoelectron and the remaining system with a photohole. The final-state energy will be the energy between the photohole and its image, according to Eq. (1), and after rearrangement for easier numerical computation

$$E_{f,\infty}(R) = \frac{e^2}{2R}\frac{\varepsilon-1}{\varepsilon} + \frac{e^2}{2R}\frac{\varepsilon-1}{\varepsilon(\varepsilon+1)}\frac{r_h^2}{R^2-r_h^2} + \frac{e^2}{2R}\frac{\varepsilon-1}{\varepsilon+1}\sum_{k=1}^{\infty}\frac{1}{k(\varepsilon+1)+1}\left(\frac{r_h}{R}\right)^{2k} \tag{3}$$

where the factor of a half stands for the self-energy or the integration of q from 0 to e. An identical expression has been formulated by Brus as the loss of dielectric solvation energy [24]. In the very large particle or bulk limit ($R \to \infty$) the first term vanishes. The second term approaches $e^2/(4h)\{(\varepsilon-1)/[\varepsilon(\varepsilon+1)]\}$ as $r_h = R - h$, which is the correct form of image potential in a planar surface. The third term still vanishes as the series approaches $\ln(R)$. Since there is no electrostatic energy in the neutral initial ground state, the measured binding energy shift of the core levels with respect to bulk will be

$$\Delta E_{\text{CL}}(R) = E_{f,\infty}(R) - E_{f,\infty}(\infty). \tag{4}$$

The final-state energy defined here arises because the organic ligands passivating the NP surfaces prevent the photohole from becoming neutralized by an electron tunneling from the metal substrate before the photoelectron escapes to far away. On the other hand, the bulk CdSe powder sample was not isolated and the photohole was readily neutralized from an electron at Fermi energy in the photoemission process. Thus the associated final-state energy should be minimal, and it allows us to take the bulk limit of final-state energy as zero in the following fit. The high frequency dielectric constant ε was calculated to become smaller as the particle size decreases [25] and their values are used here.

Fig. 3(a) compares the measured energy shift relative to bulk for Cd $3d_{5/2}$ and the interior component of Se 3d core levels of CdSe NPs with a model calculation from Eq. (4) with a vanishing bulk final-state shift (thin solid curve). Since the photon energy was tuned to have a small electron mean free path, most photoelectrons came from the surface region. We model the photohole position at $r_h = R - 3.6$ Å which gives the best fit to the data and the agreement is excellent. The shift becomes larger as the photohole position gets closer to the surface. A range of +/−1 Å variation around $r_h = R - 3.6$ Å results in approximately +0.06/−0.04 eV in the calculated shift. This value of 3.6 Å is slightly larger than the Cd–Se bond length of 2.63 Å and is reasonable because the second layer contributes most to the interior component of Se. For Cd $3d_{5/2}$ the surface component was unresolved from the interior component resulting in a slightly larger shift than that for Se as clearly shown. A much poorer fit with an unphysical photohole position of 0.8 Å would be obtained if the planar image potential is used as the bulk limit.

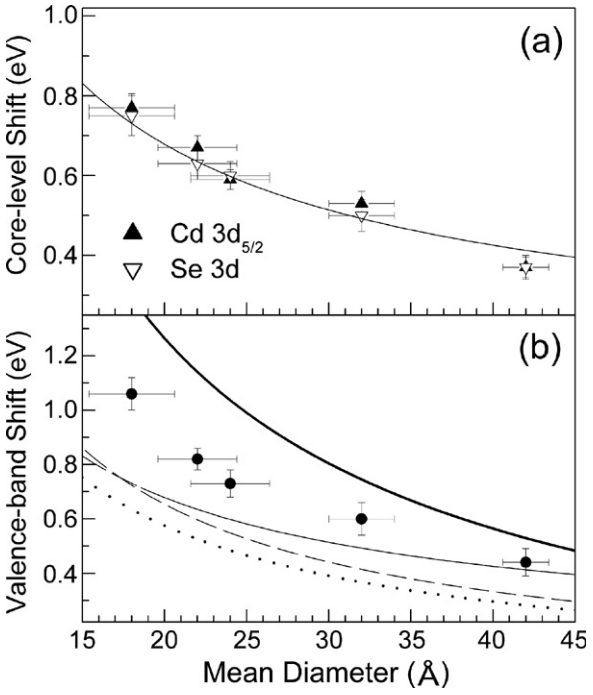

Fig. 3. Energy shifts of (a) the core level and (b) valence-band edge for TOPO/HDA capped CdSe NPs versus the mean diameter. The horizontal error bars specify the size distribution while the vertical error bars indicate the measurement uncertainty. The thin solid curve is the calculated shift by Eq. (4) with a vanishing bulk final-state shift with the photohole located at a position of $R - 3.6$ Å. The dashed curve is calculated assuming the photohole weighted by a $1S$ wave function. The dotted curve is calculated assuming the photohole located at the center. The thick solid curve is the calculated final-state shift (dashed curve) plus the initial-state shift due to quantum confinement calculated in Ref. [25].

The measured valence-band shifts are presented in Fig. 3(b) and they are always larger than the corresponding core-level shifts. Final-state shift of the valence-band edge should be different from that of the core levels because the valence edge hole wave function penetrates deeper into the interior of the NPs [25]. We anticipate that the calculated final-state shift of the valence band should be smaller than that of the core levels because the core hole is closer to the surface. However, this expected shift difference is in the opposite direction to the experimental observation. Following Ref. [24] we may model the hole $1S$ wave function as $\sin(\pi r/R)/r$ as in an infinite well for simplicity. The averaged final-state shift is shown as the dashed curve. If a step well is used the hole wave function should have more weight closer to the surface. The fitted core hole final-state shift should serve as the higher limit and is reproduced as the thin solid curve. The lower limit of the final-

state shift is obtained if the photohole is located at the center and is represented as the dotted curve. It is obvious that the pure final-state effect underestimates the valence-band edge shift. We expect an additional shift due to quantum confinement as the initial-state effect. The simplest form is the kinetic energy term in a quantum confinement well as described in the pioneering work by Brus [1], which has been used with qualitative success to explain the shift in CdS NPs [11]. More recently, Wang and Zunger calculated the electronic structure of surface-passivated wurtzite CdSe quantum dots with four sizes using a semiempirical pseudopotential method (SEPM) [25]. They show that the valence-band maximum shifts to lower energy compared to bulk CdSe as the NP becomes smaller.

The correct description for the total shift of the valence-band edge with particle size should include both the initial-state and final-state shifts as

$$\Delta E_{\mathrm{VB}}(R) = \Delta E_{\mathrm{SEPM}}(R) + \overline{\Delta W(R)} \tag{5}$$

where $\Delta E_{\mathrm{SEPM}}(R)$ is extracted from the predicted energy shifts with size by SEPM [25] and $\overline{\Delta W(R)}$ is the average of Eq. (3) over the wave function of the hole in the NP [11,24]. The thick solid curve in Fig. 3(b) is the plot of Eq. (5) using the infinite well wave function. It appears to be an overestimation compared to the measured shifts, even if either the upper or lower limit of the final-state shift is used. This discrepancy is larger for the smaller particles. We emphasize here that the amount of final-state shift is different in (the interior component of) the core levels and the valence-band edge. It can be seen in Fig. 3(b) that the final-state shift of the valence-band state is smaller than that of the core levels in our measurement size range and the disagreement becomes larger for the larger NPs. Therefore, if we take the difference of the measured energy shift of the valence-band edge and that of the core levels to represent the initial-state shift or quantum confinement change of the valence-band edge as was done in the literature [9] the values would be an underestimate particularly for the larger NPs.

A number of reasons can be discussed about the deviation. One may suspect the approximation of the prolate shape (aspect ratio of 1.2–1.3) of NPs by a sphere may result in an error in the initial state. However, the deviation of a prolate spheroid from the averaged sphere will always lead to an increase of the quantum confinement and larger initial-state shift, opposite to the experimental observation. Another point is that the presence of stacking faults in NPs is experimentally observed [2] but not considered in the calculation. However, a calculation of CdSe quantum dots in both wurzite and zinc-blende structures does not show a significant change in exciton energies [26]. Thus stacking fault seems to be unable to explain such a discrepancy. The third possibility is that a lattice contraction of up to 1% and structural disorder were observed experimentally [18, 22] while the calculation assumes a truncated bulk with bulk lattice constant. A theoretical study of CdS clusters indicates a reduction of band gaps by 0.11 eV assuming 1.4% lattice contraction [27]. These may explain the discrepancy between experiment and theory. Finally we note that it has been reported for the Si NPs that the calculated initial-state valence-band shifts using a pseudopotential method are larger than the measured values, similar to our finding on the CdSe NPs [9].

4. Conclusions

By means of photoemission spectroscopy, we have studied the size-dependent energy shift of the core levels and valence-band edges for organics capped CdSe NPs ranging in mean diameters from 18 to 42 Å, with respect to bulk CdSe. A final-state effect model, based on the electrostatic interaction between the photohole and the dielectric background, is invoked to elucidate the experimental results for the observed core-level shifts. For the valence-band edge both the final-state and initial-state shifts should be considered. However, the initial-state shift due to quantum confinement extracted from a pseudopotential calculation shows an increasing deviation with decreasing particle size. It is possibly due to the lattice contraction in the NPs neglected in the calculation. Our analysis shows that a detailed understanding of the measured photoemission shift has to consider the final-state effect and its difference between the core level and valence band.

Acknowledgements

One of us (P.J.W.) is grateful to Dr. Tun-Wen Pi for guidance in the photoemission experiments and Meng-Ting Hsieh for help in sample preparation and useful discussions. This work was supported by National Science Council, Taiwan, under Grants No. NSC 94-2122-M-213-017 and NSC 94-2112-M-213-016.

References

[1] L.E. Brus, J. Phys. Chem. 90 (1986) 2555.
[2] C.B. Murray, D.J. Norris, M.G. Bawendi, J. Am. Chem. Soc. 115 (1993) 8706.
[3] X. Peng, J. Wickham, A.P. Alivisatos, J. Am. Chem. Soc 120 (1998) 5343.
[4] M.C. Schlamp, X.G. Peng, A.P. Alivisatos, J. Appl. Phys. 82 (1997) 5837.
[5] H. Mattoussi, L.H. Radzilowski, B.O. Dabbousi, E.L. Thomas, M.G. Bawendi, M.F. Rubner, J. Appl. Phys. 83 (1998) 7965.
[6] M.J. Bowers II, J.R. McBride, S.J. Rosenthal, J. Am. Chem. Soc. 127 (2005) 15378.
[7] M. Bruchez, M. Moronne, P. Gin, S. Weiss, A.P. Alivisatos, Science 281 (1998) 2013.
[8] W.C.W. Chan, S.M. Nie, Science 281 (1998) 2016.
[9] T. van Buuren, L.N. Dinh, L.L. Chase, W.J. Siekhaus, L.J. Terminello, Phys. Rev. Lett. 80 (1998) 3803.
[10] P. Zhang, T.K. Sham, Phys. Rev. Lett. 90 (2003) 245502.
[11] V.L. Colvin, A.P. Alivisatos, J.G. Tobin, Phys. Rev. Lett. 66 (1991) 2786.
[12] K.S. Liang, W.R. Salaneck, I.A. Aksay, Solid State Commun. 19 (1976) 329.
[13] H.G. Boyen, A. Ethirajan, G. Kästle, F. Weigl, P. Ziemann, G. Schmid, M.G. Garnier, M. Büttner, P. Oelhafen, Phys. Rev. Lett. 94 (2005) 16804.
[14] G.K. Wertheim, S.B. DiCenzo, S.E. Youngquist, Phys. Rev. Lett. 51 (1983) 2310.
[15] G. Makov, A. Nitzan, L.E. Brus, J. Chem. Phys. 88 (1987) 5076.
[16] M. Seidl, K.H. Meiwes-Broer, M. Brack, J. Chem. Phys. 95 (1991) 1295.
[17] P. Reiss, J. Bleuse, A. Pron, Nano Lett. 2 (2002) 781.
[18] P.J. Wu, et al., unpublished.
[19] W.W. Yu, L. Qu, W. Guo, X. Peng, Chem. Mater. 15 (2003) 2854.

[20] S.W. Gaarenstroom, N. Winograd, J. Chem. Phys. 67 (1977) 3500.
[21] H. Borchert, D.V. Talapin, C. McGinley, S. Adam, A. Lobo, A.R.B. de Castro, T. Moller, H. Weller, J. Chem. Phys. 119 (2003) 1800.
[22] K.S. Hamad, R. Roth, J. Rockenberger, T. van Buuren, A.P. Alivisatos, Phys. Rev. Lett. 83 (1999) 3474.
[23] E. Agostinelli, C. Battistoni, D. Fiorani, G. Mattogno, M. Nogues, J. Phys. Chem. Solids 50 (1989) 269.
[24] L.E. Brus, J. Chem. Phys. 79 (1983) 5566.
[25] L.W. Wang, A. Zunger, Phys. Rev. B. 53 (1996) 9579.
[26] B. Zorman, M.V. Ramakrishna, R.A. Friesner, J. Phys. Chem. 99 (1995) 7649.
[27] M.V. Rama Krishna, R.A. Friesner, J. Chem. Phys. 95 (1991) 8309.